Electronic Supplementary Information (ESI) for

Carbon-coated, methanol-tolerant platinum/graphene catalysts for oxygen reduction reaction with excellent long-term performance

Wenya Song [a,‡], Zhongxin Chen [a,‡], Chao Yang [a,‡], Ziping Yang [a], Jiapo Tai [a], Yulong Nan [a] and Hongbin Lu [a,*]

State Key Laboratory of Molecular Engineering of Polymers, and Department of Macromolecular Science, Fudan University, 220 Handan Road, Shanghai, 200433, China. Tel/Fax: 86-21-5566 4589. To whom correspondence should be addressed: hongbinlu@fudan.edu.cn.

‡ These authors contributed equally.

This PDF includes:

---

1. Experimental Section for the Preparation of G/Pt Catalysts :

1.1 Chemicals:

Graphite powder 8099200 (120 μm) was purchased from Qingdao BCSM Co., 98% H_2SO_4, 65% HNO_3, 30% H_2O_2, glucose, hexachloroplatinic acid (H_2PtCl_6•$6H_2O$), poly (vinyl pyrrolidone) (PVP, K-30, M_w =40,000) were purchased from Sinopharm Chemical Regent Co., sodium nitrate was purchased from Shanghai Qiangshun Chemical Co., $KMnO_4$, ethanol were purchased from Shanghai Zhenxin Chemical Co., isopropanol was purchased from Jiangsu Tongsheng Chemical Co., α-Al_2O_3 (0.3 μm) and γ-Al_2O_3 (0.05 μm) were purchased from CH Instruments Inc., 5 wt% Nafion® solution was purchased from Alfa Aesar. All chemicals were used as received. Deionized water was used in all experiments.

1.2 Preparation of G/Pt and Glu-G/Pt Catalysts:

Graphene oxide (GO) was prepared by Hummers method. In a typical experiment, glucose (2000 mg), PVP (50 mg) and H_2PtCl_6•$6H_2O$ aqueous solution (1 mL, 25 mg mL^{-1}) were added to 50 mL GO aqueous solution (0.5 mg mL^{-1}). The mixture was stirred magnetically for 15 min, and then sonicated for 20 min to obtain a uniform solution. Hydrothermal treatment was carried out in a 100 mL autoclave at 180 ^oC for 8h. The resulting dark black solution was purified by centrifugation at 10,000 rpm for 20 min using DI water (8 ~ 10 times) and ethanol (at least 10 times) until the supernatant was colorless. The as-obtained Glu-G/Pt catalyst was then freeze-dried to constant weight. Bare-G/Pt catalyst was obtained by the same procedure without the addition of glucose. Control groups (bare-G and Glu-G) were prepared without the addition of H_2PtCl_6•$6H_2O$ aqueous solution.

1.3 Carbonization of G/Pt and Glu-G/Pt Catalysts:

For the carbonization, Glu-G/Pt catalyst (~ 4 mg) was added to a ceramic crucible (10 mL) and then transferred to a tube furnace (SGL-1200, Shanghai Daheng Optical and Fine Mechanics Co., Ltd., China) at 700 °C for 3 h where a continuous N_2 flow was introduced at a rate of 50 L h^{-1}, and the heating rate was set at 10 °C min^{-1}. The product (C-Glu-G/Pt) was cooled down to room temperature in nitrogen and then stored under vacuum. C-G/Pt catalyst was obtained by the same procedure.

1.4 Characterizations of Physico-chemical Properties:

Water bath sonication was performed with SCS 5200 sonicator (20 kHz/700 W). Transmission electron microscopy (TEM, JEM-2100F and Tecnai G^2 20 Twin, both operating at 200 kV) was used to observe morphology of G/Pt-based catalysts at different magnifications. All samples for imaging were prepared by depositing ethanol dispersion (0.05 mg mL^{-1}) on a holey copper grid. Dark field image was taken by a Tecnai G^2 20 Twin TEM with a spatial resolution of 0.2 nm. Atomic force micrographs (AFM) were acquired using a Multimode Nano 4 in tapping mode. Samples for AFM examination were prepared by depositing ethanol dispersion of G/Pt-based catalysts (0.05 mg mL^{-1}) on freshly cleaved mica surfaces. X-ray photoelectron spectra (XPS) was carried out on an

AXIS UltraDLD system (Kratos) with monochromatic Al K_α radiation (hv = 1486.6 eV). The microstructure of Glu-G/Pt catalysts were observed with S-4800 high resolution field emission scanning electron microscopy (FE-SEM). Energy dispersive analysis of X-ray (EDX) was performed on S-4800 FE-SEM with a Bruker QUANTAX 400 detector. X-ray diffraction tests were carried out using PANalytical. X'Pert PRO X-ray diffractometer with Cu K_α radiation (λ = 1.54 Å) at a scanning rate of 1.2 ° min^{-1} in 2θ range from 10 to 80°, operating at 40 kV and 40 mA. Fourier transform infrared spectroscopy (FT-IR) was recorded on a NEXUS 670 spectrometer at room temperature over a frequency range of 4000 - 625 cm^{-1}. Thermogravimetric analysis (TGA) was conducted with Pyris 1 TGA and air as a purge gas, from ambient temperature to 800 °C at a heating rate of 20 °C min^{-1}. All samples were ground to powder prior to tests to ensure adequate heat conduction. Raman spectra were acquired using a multi-channel confocal microspectrometer with a laser wavelength of 631 nm (Dilor LABRAM-1B). Freshly prepared powders were used for XRD and Raman.

1.5 Electrochemical Measurements:

1.5.1 Cyclic voltammograms (CV) measurements:

CV patterns were recorded on a CHI 660E electrochemical workstation (CHI Inc., United States) at room temperature in a three-electrode cell using a Ag/AgCl electrode and a Pt wire as the reference and the counter electrode. A glassy carbon (GC) electrode for working electrode (3 mm diameter) was polished using 0.3 and 0.05 μm alumina slurries, followed by washing with water and ethanol. The catalyst ink was prepared by dispersing 2.0 mg catalyst in 200 μL isopropanol. A dilute Nafion® solution (200 μL, 5 wt % ethanol solution) was mixed and sonicated for 10 min. A quantity of 2 μL of the mixture was pipetted onto the GC electrode surface. The coating was then dried at room temperature in air. Typically, the electrolyte (0.5 M H_2SO_4 or 0.1 M $HClO_4$, with or without 0.5 M methanol) was either saturated by N_2 or O_2 for nearly 30 min. CV curves in 0.1 M $HClO_4$ at various methanol concentrations were also collected under O_2 at 1600 rpm with a scan rate of 50 mV s^{-1}.

1.5.2 Rotating disk electrode (RDE) experiments:

To compare the catalytic activities for ORR under different concentrations of methanol, the RDE experiments were carried out on a CHI 605 electrochemical workstation (CHI Inc., United States) in a three-electrode cell using a reversible hydrogen electrode (RHE) and a Pt gauze as the reference and the counter electrode. The GC working electrode (5 mm diameter) was prepared as described, except 5μL of the mixture was used. The polarization curves were obtained between 0.1 and 1.1 V (*vs.* RHE) and various rotating speeds with a scan rate of 10 mV s^{-1} at room temperature. LSV measurements were conducted in O_2-saturated 0.1 M $HClO_4$ at various methanol concentrations with a scan rate of 5 mV s^{-1} at room temperature.

1.5.3 Cycling performance by CV measurement:

The reproducible CV patterns after consecutive scanning were recorded between -0.2 and 1.0 V (*vs.* Ag/AgCl) at a scan rate of 50 mV s^{-1} for comparison. The long-term stability

of the catalysts was evaluated by a continuous 6,000 or 10,000 potential cycling in N_2 or O_2-saturated electrolyte (0.5 M H_2SO_4 with or without 0.5 M methanol). To exclude the influence of possible methanol consumption during cycling test, we changed the electrolyte solution at every 2,000 cycles.

2. TEM Investigation on the Morphology of G/Pt Catalysts:

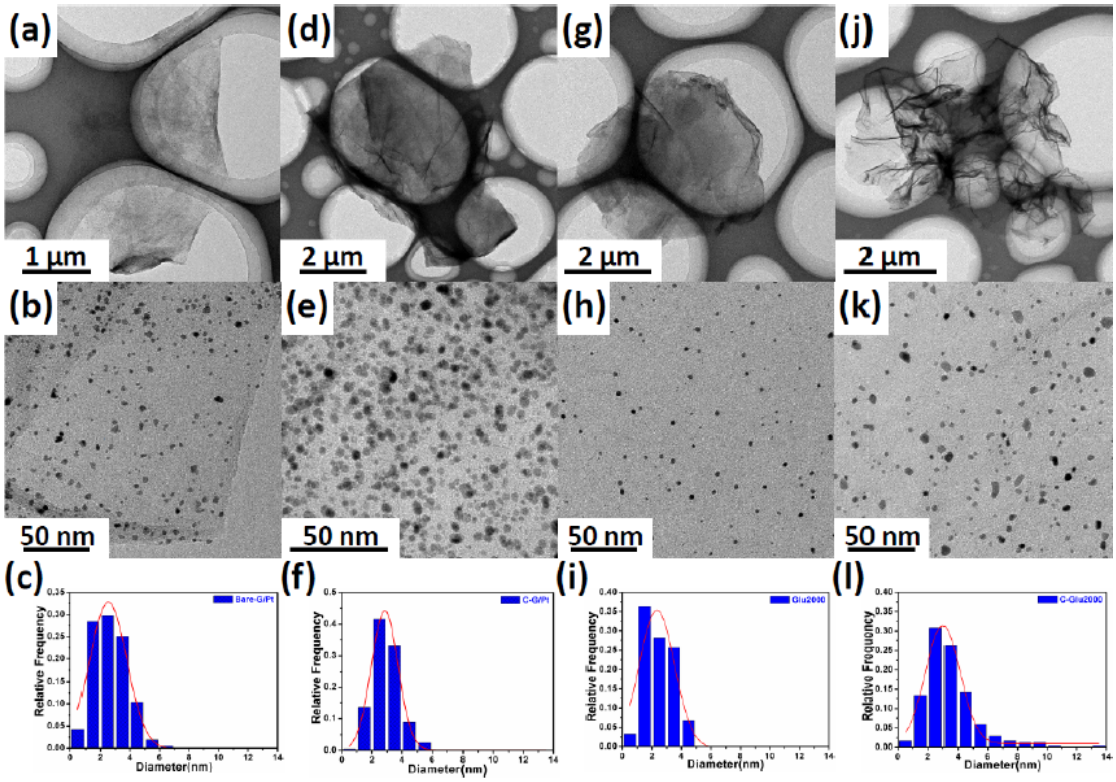

Figure S1. TEM images and corresponding NPs size distribution of G/Pt catalysts. (a-c) bare-G/Pt; (d-f) C-G/Pt; (g-i) Glu-G/Pt and C-Glu-G/Pt (j-l). All TEM images reveal the uniform distribution of Pt NPs on GNs with a mean size of ~ 3 nm.

3. FESEM Images and EDX Spectrum of G/Pt Catalysts:

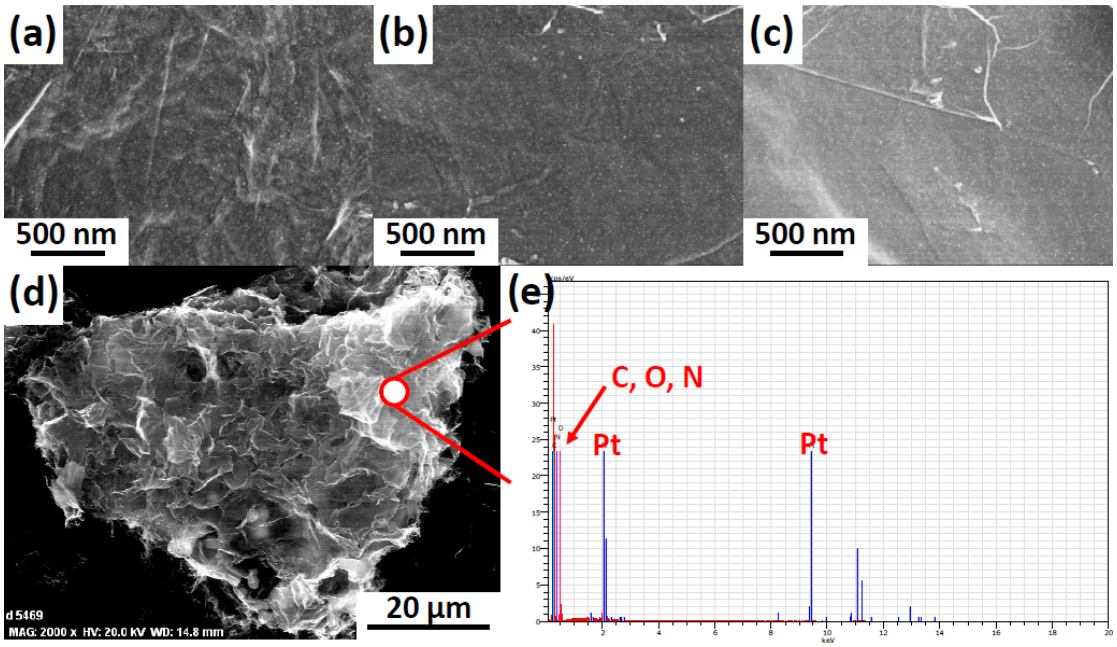

Figure S2. FESEM images of (a) bare-G/Pt, (b) Glu-G/Pt, (c, d) C-Glu-G/Pt and corresponding EDX spectrum of (d). No visible aggregation of Pt NPs is found in G/Pt catalysts.

4. Characterization of Commercial 20 wt% Pt/C Catalyst:

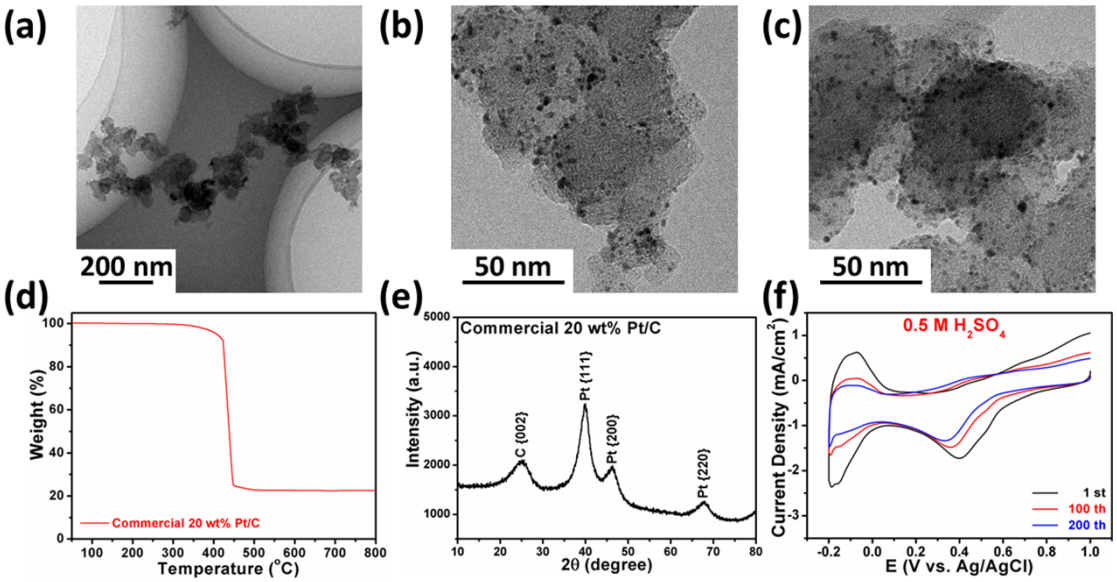

Figure S3. TEM images, chemical characterization and cycling performance of commercial 20 wt% Pt/C catalyst. (a-c) TEM images at different magnfications, the size of Pt NPs is ~ 3.5 nm; (d) TGA curves under air with a Pt loading of 22.5 wt%; (e) XRD patterns and (f) CV patterns under O_2 at the 1st, 100th and 200th cycle revealling the poor durability of commercial Pt/C catalysts.

5. Chemical Composition of G/Pt Catalysts:

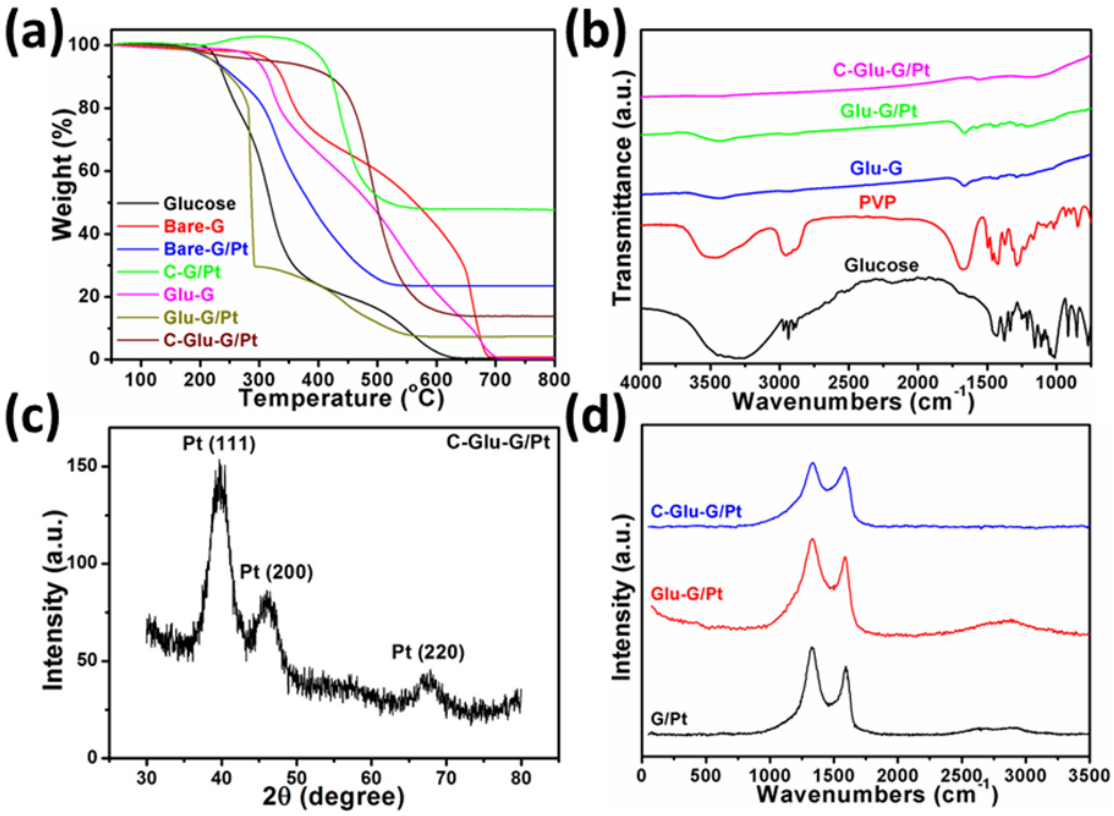

Figure S4. (a) TGA curves under air, (b) FT-IR spectra, (c) XRD patterns and Raman spectra (d) of G/Pt catalysts to verify the change in chemical composition before/after carbonization.

The Pt loading of bare-G/Pt, C-G/Pt, Glu-G/Pt and C-Glu-G/Pt are 23.4, 47.6, 7.4, 13.7 wt%, respectively. The unusual TGA curve of Glu-G/Pt was examined at least 3 times and may result from the loose attachment of glucose molecules. The increased sample weight of C-G/Pt is probably due to the absorption of O_2 gas at a moderate temperature. As a result of the removal of residual functional groups and attached PVP/glucose molecules, the Pt loading of catalysts increases after carbonization. One should point out that the Pt-loading of C-G/Pt is 3.5 times greater than C-Glu-G/Pt, where the latter is roughly half of commercial Pt/C catalysts (22.5 wt%). In this regard, the mass activity of C-Glu-G/Pt should be higher than the others, since we used current density to compare their ORR activities and the same feed amount was used for all catalysts (~ 10 μg).

In **Fig. S4b**, the content of oxygen-containing groups is greatly reduced after two steps reduction (hydrothermal treatment and high temperature carbonization). This is also comfirmed by Raman spectra in **Fig. S4d**, where a decreased I_D/I_G ratio (1.287, 1.208 and 1.076) for G/Pt, Glu-G/Pt and C-Glu-G/Pt catalysts was found. It is well-known that (110), (111) and (100) are the most common stable planes for Pt-based catalysts, with activities increasing in the order Pt (100) << Pt (111) < Pt (100). In **Fig. S4c**, representative diffraction peaks of Pt [(111), (200), (220)] are distinctly observed in the XRD patterns of Glu-G/Pt, which means that Pt forms the face-centered cubic (fcc) crystal structure. Therefore, the difference in catalytic activity/methanol tolerance is not arised from the shape or crystal structure. The presence of weak peak at ~25° corresponds to C (002).

6. Deconvolution Results of C_{1s}, N_{1s}, O_{1s}, and Pt_{4f} Core-level Spectra:

Table S1. Chemical compositions of G/Pt catalysts from XPS spectra. [a]

		Carbon 1s				Nitrogen 1s		Oxygen 1s		
	Species	C-C	C-N/C-O	C=O	O-C=O	amide	amine	amide	C=O	C-O
	Energy	284.72	285.97	287.51	289.00	399.60	401.45	531.20	532.50	533.50
Glu-G/Pt	FWHM	1.50	1.50	1.50	1.50	1.50	1.50	1.80	1.80	2.00
	Atom%	57.0	27.6	12.9	02.5	87.0	13.0	42.3	35.2	22.5
	Energy	284.71	285.90	287.60	-	-	400.47	-	531.10	533.03
C-Glu-G/Pt	FWHM	1.14	1.50	1.50	-	-	3.33	-	2.15	2.50
	Atom%	80.7	16.4	02.9	-	-	100	-	26.9	73.1

		Platinum $4f_{7/2}$			Platinum $4f_{5/2}$			Survey		
	Species	Pt	PtO	PtO_2	Pt	PtO	PtO_2		Glu-G/Pt	C-Glu-G/Pt
	Energy	70.97	72.22	73.58	74.33	75.46	76.80			
Glu-G/Pt	FWHM	1.25	1.30	1.30	1.30	1.30	1.30		Atom%	Atom%
	Atom%	43.9	10.1	03.2	31.2	08.8	02.8	C_{1s}	78.40	95.47
	Energy	71.50	72.76	74.12	74.88	76.03	77.35	N_{1s}	04.83	01.50
C-Glu-G/Pt	FWHM	1.19	1.20	1.20	1.20	1.20	1.20	O_{1s}	16.68	02.90
	Atom%	48.1	08.6	03.4	29.6	07.4	02.9	Pt_{4f}	00.09	00.13

a) Fitting parameters of C_{1s}, N_{1s} & O_{1s} spectra are fixed due to the negligible influence of Pt atoms on peak shifts.

7. CV Patterns and LSV Curves of C-Glu-G/Pt and Commercial Pt/C Catalysts at Various Methanol Concentrations:

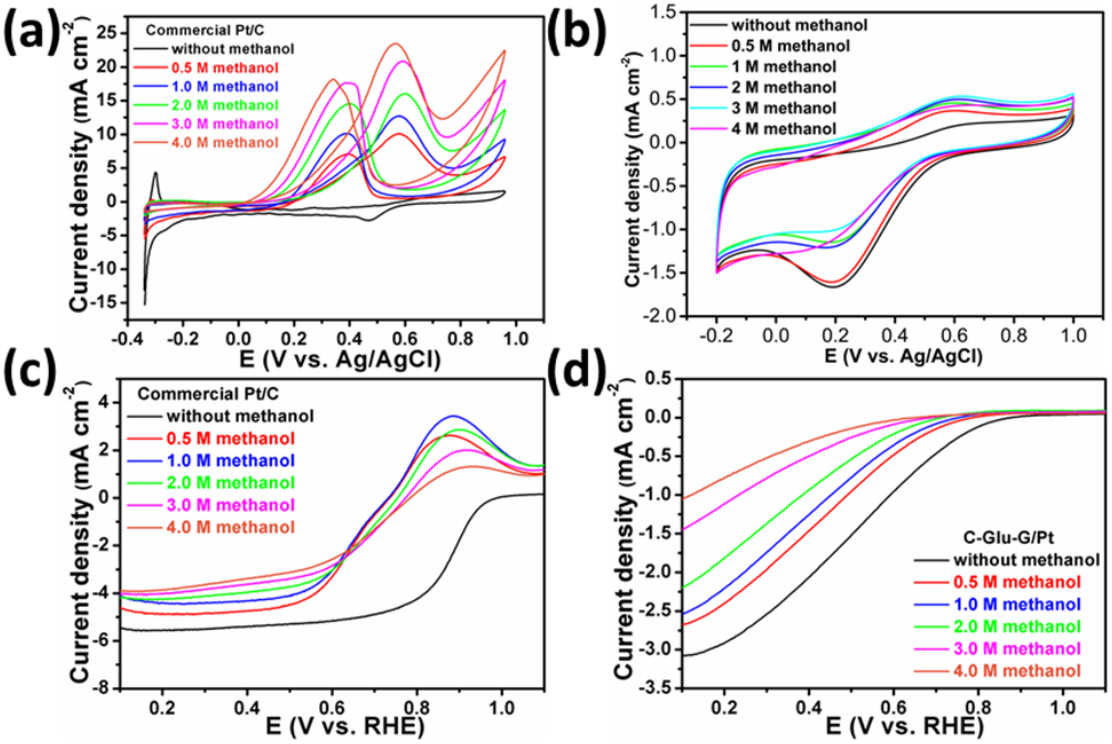

Figure S5. Methanol tolerance of commercial Pt/C and C-Glu-G/Pt catalysts: (a, b) CV curves in 0.1 M $HClO_4$ at various methanol concentrations under O_2 at 1600 rpm. Scan rate: 50 mV s^{-1}, temperature: 25 ^oC. (c, d) LSV curves in O_2-saturated 0.1 M $HClO_4$ at various methanol concentrations. Scan rate: 5 mV s^{-1}, temperature: 25 ^oC.

8. CV patterns of G/Pt Catalysts under N_2 and O_2 before Carbonization:

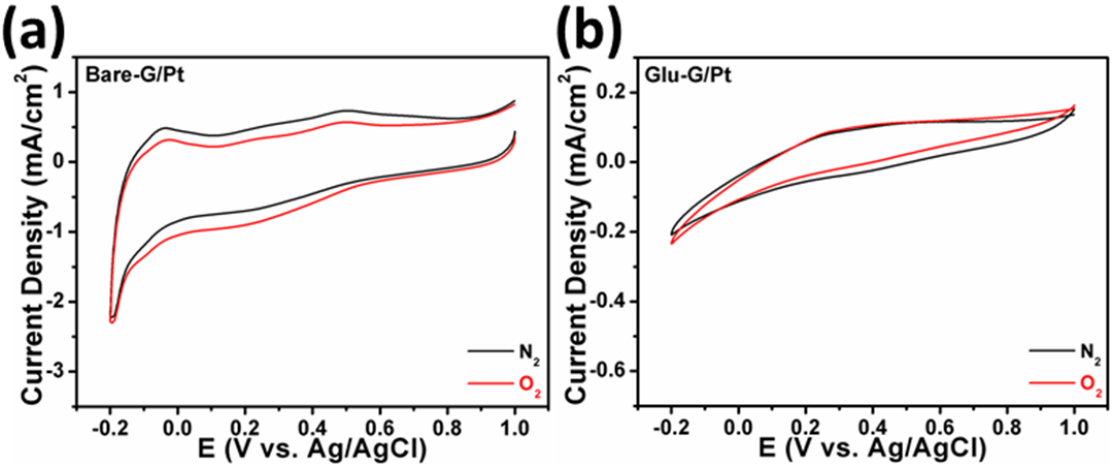

Figure S6. CV patterns of bare-G/Pt and Glu-G/Pt catalysts under N_2 and O_2 at a scan rate of 50 mV s^{-1}, electrolyte: 0.5 M H_2SO_4. The poor performance of bare-G/Pt is ascribed to the relatively low conductivity and the attachment of PVP molecules on Pt NPs. Glu-G/Pt shows nearly no ORR activity since the Pt NPs are fully covered by the carbon layer (PVP or glucose).

9. Cycling Performance of G/Pt Catalysts under N_2 and Their Morphology:

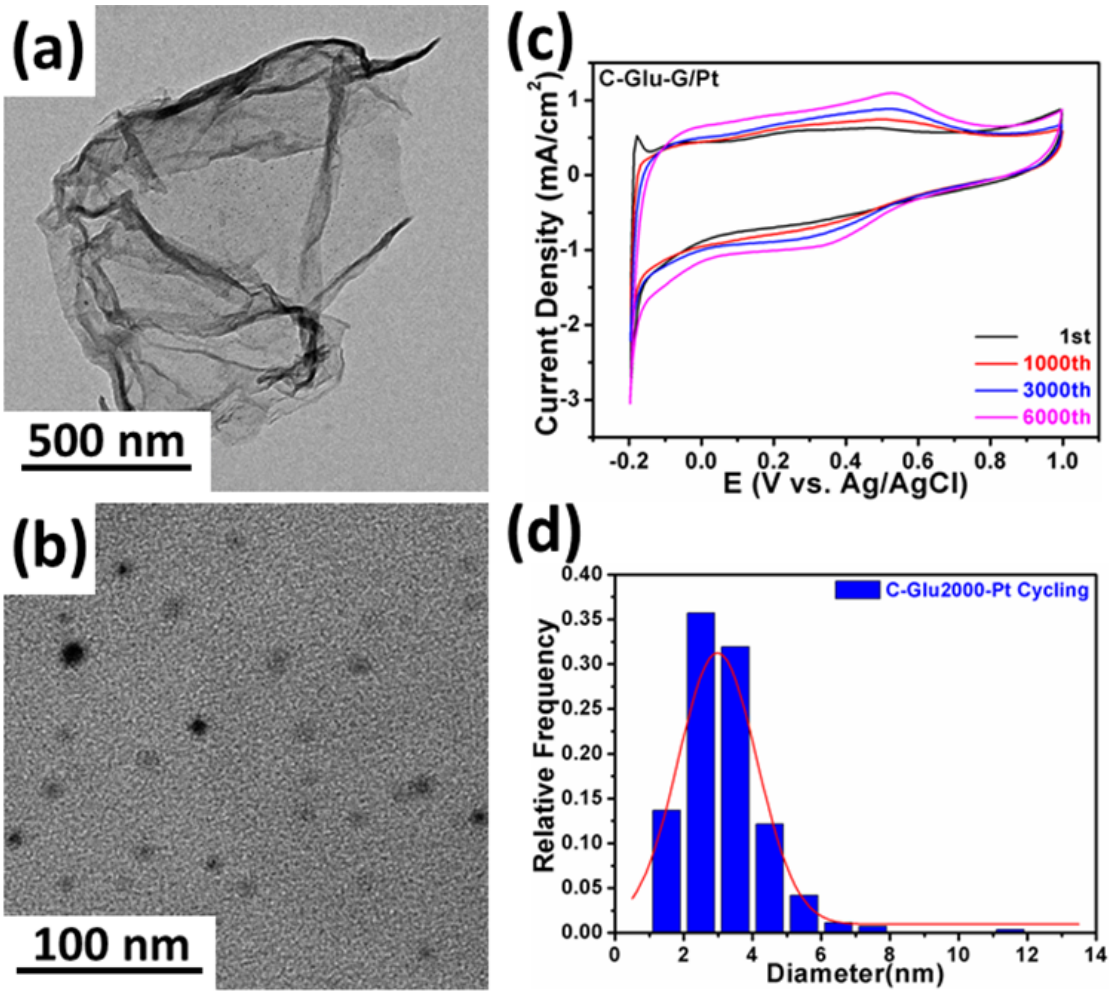

Figure S7. Cycling performance of C-Glu-G/Pt catalyst under N_2 at a scan rate of 50 mV s^{-1}, electrolyte: 0.5 M H_2SO_4; Representative TEM images and corresponding NPs size distribution (from > 100 NPs, ~ 3 nm) after cycling test under N_2.

We also performed a continuous 6000 potential cycling under N_2 to further verify the effect of carbon-coating. As shown in **Fig. S7c**, the 6000th CV pattern of C-Glu-G/Pt suggests a higher electrochemical activity (higher current density and larger area). This is consistent with the cycling tests under O_2, which may cause from the slow corrosion of carbon layer and increased surface area of Pt NPs. Unfortunately, we could not estimate the electrochemical active specific surface area (ESA) of platinum from **Fig. S7c**, as a result of the lack of hydrogen absorption/desorption peaks. Instead, we took high resolution TEM images to demonstrate the protection of carbon layer. It is seen that Pt NPs uniformly distributed on GN after cycling tests in **Fig. S7a**. Furthermore, the mean size of NPs (~ 3 nm) is nearly unchanged after long-term cycling, indicating an excellent stability in comparison with commercial Pt/C catalysts (See **Ref S1**).

10. TGA curves of PVP and glucose in N_2 and air:

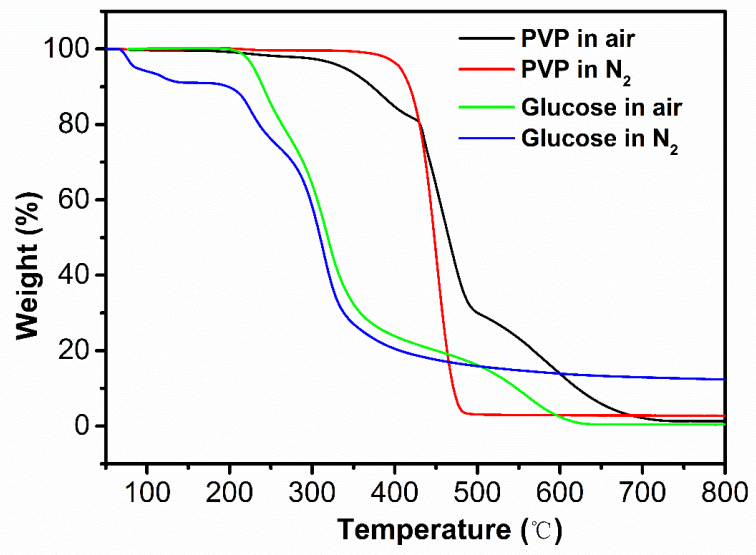

Figure S8. TGA curves of PVP and glucose in N_2 and air at a rate of 10 °C min^{-1}.

The decomposition temperature of PVP and glucose are about 465 °C and 220 °C in N_2 with a finally residual weight ~ 3% and 13%, respectively. In addition, PVP and glucose in air have been almost completely removed, with a residual weight only ~ 0.5%. Therefore, PVP and glucose should be completely removed or converted into a carbon coating layer after carbonization treatment at 700 °C for 3 h.

References:

1. Xingwen Yu, Siyu Ye, Recent advances in activity and durability enhancement of Pt/C catalytic cathode in PEMFC Part I. Physico-chemical and electronic interaction between Pt and carbon support, and activity enhancement of Pt/C catalyst, *Journal of Power Sources*, 2007, **172**, 133-144;